

# Rheological properties of sodium pyrophosphate modified bentonite suspensions for seepage control



Jisuk Yoon <sup>\*,a</sup>, Chadi S. El Mohtar <sup>b</sup>

<sup>a</sup> Fugro Consultants Inc., 6100 Hillcroft, Houston, TX 77081, United States

<sup>b</sup> Department of Civil, Architectural and Environmental Engineering, The University of Texas at Austin, Austin, TX 78712-0280, United States

## ARTICLE INFO

### Article history:

Received 17 August 2013

Received in revised form 13 June 2014

Accepted 14 June 2014

Available online 27 June 2014

### Keywords:

Bentonite suspension

Permeation grouting

Rheology

Sodium pyrophosphate

Vane

Yield stress

## ABSTRACT

The placement of plastic fines such as bentonite into pore spaces of granular soil deposits is one of the effective methods to control the seepage problem. For such an application, bentonite needs to be delivered into soils in forms of concentrated suspensions without disturbing the original soil matrix using low injection pressures (permeation grouting). However, the low penetrability of the concentrated suspensions through soils limits their practical applicability for large-scale seepage control in the field. In order to increase the penetration distance, the initial mobility of the suspensions should be increased; however, the suspensions need to maintain their thixotropic nature to reduce the washout probability of the suspensions from the treated soils over time. The objective of this study is to investigate the rheological properties of concentrated bentonite suspensions, modified with sodium pyrophosphate (SPP), for evaluating a possible application of the modified suspensions in seepage control through permeation grouting. In this paper, yield stress and apparent viscosity of the SPP modified bentonite suspensions measured by the stress ramp technique are presented. Bentonite suspensions with the clay contents of 5, 7.5, 10, and 12% (by total weight of suspension; W/B (weight ratio of water (W) and bentonite (B)) = 19, 12.3, 9, and 7.3) were tested at various SPP concentrations (0 to 7% by weight of dry bentonite). Moreover, the time-dependent behavior of the suspensions was evaluated through measuring the yield stress at various resting times (0 to 45 days). The results show that the initial yield stresses are reduced to approximately zero and apparent viscosities decrease approximately 70–90% with the addition of 2, 3, and 4% SPP for the 7.5, 10, and 12% suspensions, respectively. The reduced yield stresses increase gradually with resting times, reaching approximately 90 to 180% of the yield stresses of the unmodified suspensions after 45 days. However, the required resting times for full recovery of yield stress increase with the increase of percentage of SPP used.

© 2014 Elsevier B.V. All rights reserved.

## 1. Introduction

Over the past years, a majority of levee failures in the United States have been induced by under-seepage through granular foundation soils underneath the top soil on which the levees were built, causing significant losses of lives and properties (Chrastowski et al., 1994; Seed et al., 2008). One of the effective methods to mitigate this phenomenon is to treat the granular foundation soils with plastic fines such as bentonite. Hwang et al. (2011) reported that the permeation of bentonite suspensions reduced the saturated hydraulic conductivity of Ottawa sand 3 to 5 orders of magnitude. This implies that the bentonite grouting could be an effective method to control seepage through granular soils once bentonite suspensions are placed in the pores of the soils. For such an application, bentonite needs to be delivered into soils in forms of concentrated suspensions by permeation (permeation grouting). However, the application of the concentrated suspensions (exceeding 5% by weight)

in seepage control is limited due to their low penetrability through soils. Therefore, the suspensions should be liquefied to increase their penetration distance. On the other hand, the increased mobility needs to be temporary, and the suspensions should start gelling rapidly over time to achieve the resistance to ground water flow and settling after permeation.

Previous researchers have widely studied the effect of the various ionic additives on bentonite suspensions (Tchillingarian, 1952; Jessen and Turan, 1961; Gonzalez and Martin-Vivaldi, 1963; Abend and Lagaly, 2000; Penner and Lagaly, 2001). Recently, Chegbeleh et al. (2009) reported that a significant amount of ethanol (30 to 50% by weight of bentonite) could liquefy the concentrated bentonite suspensions (6 to 14% by weight of total suspension). While the various ionic additives tend to increase the initial mobility of bentonite suspensions, the time-dependent behavior of the treated suspensions depends on the type of the additive. Bentonite suspensions treated with sodium hydroxide produced substantially high mobility (low yield stress and viscosity) compared to the untreated suspensions after 24 h (Gonzalez and Martin-Vivaldi, 1963). Tchillingarian (1952) observed complete

\* Corresponding author. Tel.: +1 713 369 5458.  
E-mail address: [JYOON@FUGRO.COM](mailto:JYOON@FUGRO.COM) (J. Yoon).

flocculation in clay suspensions treated with a polyphosphate (sodium hexametaphosphate) compared to the complete deflocculation in clay suspensions treated with sodium hydroxide after 3 days.

The 3-D network structures in bentonite suspensions, either a card-house (van Olphen, 1977) or band-like structure (Norris, 1954; Weiss and Frank, 1961), are continuous and integrated under appropriate solution conditions (pH, type, and concentration of electrolyte). Cryo-SEM micrographs (Morris and Žbik, 2009) revealed that the network structures in smectite suspensions consisted of aggregated individual particle platelets arranged in a combination of sandwiched edge-edge aggregates of the stacks. The inter-aggregate bonds contribute to form the 3-D networks in the suspensions and control the mobility of the suspensions. The inter-aggregate bonds are broken when the applied stress is beyond yield stress. Since these types of bonds are partially reversible, most of these bonds are gradually recovered over time (Nguyen and Boger, 1985). However, the network structures and time-dependent rheological behavior of the bentonite suspensions treated with ionic additives are not well documented in the literature.

The objective of this study is to investigate the rheological properties of concentrated bentonite suspensions modified with an ionic additive, sodium pyrophosphate (SPP), for evaluating a possible application of the modified suspensions in seepage control by permeation grouting. This study presents the rheological properties of the SPP modified bentonite suspensions, focusing on their time-dependent behavior. The SPP was selected to control the mobility of the concentrated bentonite suspensions because, contrasting to sodium hydroxide and sodium silicate, the SPP displays pronounced dispersing capability (Tchillingarian, 1952; Penner and Lagaly, 2001) and may allow gradual decrease in mobility with time; both of which are desirable properties for the proposed application. The flow behavior of the bentonite suspensions is characterized by the yield stress and apparent viscosity. Specifically, yield stress is utilized to illustrate the time-dependent behavior of the modified bentonite suspensions because yield stress provides information on the strength of the flocculated 3-D network structures and a phase transition from liquid-like to solid-like behavior of the suspensions (Goh et al., 2011; Jeong, 2013). The yield stress is also a critical grouting design parameter to evaluate propagation distance and post-grouting stability of grouts (Cambefort, 1977; Gustafson and Stille, 1996; Axelsson, 2006; Liu and Neretnieks, 2006; Axelsson and Gustafson, 2007; Axelsson et al., 2009). Similar to yield stress, beyond a threshold shear rate, the apparent viscosity starts being degraded such that the behavior of the bentonite suspension transits from solid-like to liquid-like. Moreover, the apparent viscosity of bentonite suspensions is directly related to the performance of grouting works (Yoon and El Mohtar, 2013b). A kinetic model is applied to evaluate the rate of time-dependent increase in 3-D networks of bentonite suspensions. Environmental Scanning Electron Microscope (ESEM) studies are presented to qualitatively investigate the change in the 3-D networks of the SPP modified bentonite suspensions with resting time.

## 2. Materials and methods

### 2.1. Materials

Wyoming sodium-bentonite (CP-200, CETCO, Wyoming, USA) was used in this study. The particles have a platy shape with an average diameter usually less than 1–2  $\mu\text{m}$  (Mitchell, 1993; Luckham and Rossi, 1999). The raw bentonite initially included large-sized impurities (>75  $\mu\text{m}$ ); therefore, the bentonite was screened through a No. 200 sieve (opening size of 75  $\mu\text{m}$ ) to minimize the impurities and their effects on the results (Abend and Lagaly, 2000; Clarke, 2008). This process produced approximately 95 wt.% of particles less than 25  $\mu\text{m}$  and 50 wt.% of particles less than 1  $\mu\text{m}$  (ASTM D422). While the presence of some additional impurities such as sodium carbonate could interfere with SPP (Alther, 1987), no further purification or gradation was applied to simulate practical mass production of material for field applications.

The pH measurements of the unmodified suspensions immediately after mixing with de-ionized water show a consistent alkalinity of the average of 9.3 with the standard deviation and coefficient of variation (COV) of 0.3 and 0.03, respectively. While the rheological behavior of bentonite suspensions can be affected by pH of the suspensions, Kelessidis et al. (2007) reported that there was little difference of pH values between the moment of mixing and full hydration (approximately 16 h) for concentrated bentonite suspensions (6.42% by weight) having pH values beyond the natural pH (approximately 9.0). Therefore, the time-dependent pH was not measured in this study. In order to determine the cation exchange capacity and specific surface area, methylene blue (MB) adsorption technique was used (Yukselen and Kaya, 2008). The specific surface area was calculated based on the method suggested by Santamarina et al. (2002). The chemical formula and molecular weight of methylene blue used are  $\text{C}_{16}\text{H}_{18}\text{ClN}_3\text{S}_3\text{H}_2\text{O}$  and 373.90, respectively. The surface area covered by a methylene blue molecule is assumed to be 130  $\text{\AA}^2$ . The properties of the sieved bentonite are summarized in Table 1.

Chemical analysis (Table 2) was performed using Philips/FEI XL30 ESEM (FEI Company, Hillsboro, OR, USA) equipped with energy diffraction analysis of X-ray (EDX) to characterize the chemical composition of the sieved bentonite powder. A Gaseous Secondary Electron (GSE) detector was utilized with frame and spot mode of the EDX. The Na/Ca molar ratio is 1.9.

Commercially available Sodium pyrophosphate decahydrate ( $\text{Na}_4\text{P}_2\text{O}_7 \cdot 10\text{H}_2\text{O}$ , purity  $\geq 99\%$ , Sigma-Aldrich, St. Louis, MO, USA) was used in the present study. Specific gravity and molecular weight of SPP are 1.8 and 446.06, respectively. A 5% SPP solution was prepared in advance and the appropriate amount of the solution was added to the water and bentonite. The pH of 5% solution measured using a JENCO 60 pH meter is 9.5. Deionized water, with constant ionic concentration of  $2 \times 10^{-5}$  mM, was used for preparing all the bentonite suspensions and SPP solution.

### 2.2. Methods

#### 2.2.1. Sample preparation

Yield stress of bentonite suspensions was measured at various bentonite contents (5, 7.5, 10, and 12%) and SPP (0 to 7%) concentrations, and resting times (0 to 45 days). The samples were prepared based on the method described in Yoon and El Mohtar (2013c). The clay fraction of bentonite suspension is determined as the weight ratio of dry bentonite to the total weight of the suspension and the concentration of SPP is calculated as the weight ratio of SPP to the dry bentonite. For fresh suspensions, the screened bentonite powder was placed in a mixing cup and thoroughly mixed with de-ionized water and a designated amount of 5% SPP solution using a high shear mixer (Hamilton Beach 950 spindle mixer) for 15 min. For samples rested for extended periods of time, the suspensions were stored in the cups specifically manufactured for this study. Mineral oil was added on top of the bentonite suspensions to reduce any evaporation from the samples, and then the cups were tightly sealed and stored in the cabinet that was free of vibration. The mineral oil was removed using an eyedropper and the surface was slightly trimmed with a straight edge prior to shearing to ensure complete removal of the oil.

**Table 1**  
Properties of Wyoming bentonite (CP-200).

|                       |      |                                    |                       |
|-----------------------|------|------------------------------------|-----------------------|
| PL                    | 38%  | CEC <sup>a</sup>                   | 91 meq/100 g          |
| LL                    | 440% | Specific surface area <sup>b</sup> | 712 m <sup>2</sup> /g |
| Gs                    | 2.7  | pH                                 | 9.3                   |
| Initial water content | 8.3% | Swelling capacity                  | 8 ml/g                |

<sup>a</sup> Methylene blue adsorption test.

<sup>b</sup> Calculated the method suggested by Santamarina et al. (2002).

**Table 2**  
Chemical analysis of Wyoming bentonite (CP-200), wt.%.

|    |       |       |      |
|----|-------|-------|------|
| O  | 53.05 | K     | 0.52 |
| Na | 2.27  | Ca    | 1.2  |
| Mg | 1.52  | Ti    | 0.15 |
| Al | 9.07  | Cr    | 0.11 |
| Si | 28.77 | Mn    | 0.2  |
| P  | 0.46  | Fe    | 2.31 |
| S  | 0.43  | Total | 100  |
| Cl | 0.09  | Na/Ca | 1.9  |

### 2.2.2. Rheological test

A Physica MCR 301 rheometer (Anton Paar, Granz, Austria) was used in this study. Vane geometry was utilized to measure the yield stress and apparent viscosity. The vane used has six blades, each with a thickness of 1 mm and a length of 16 mm. The vane radius is 11 mm, resulting in a 3.46 mm gap between the cup and the vane. The cups manufactured for long-term resting of samples are 80 mm in length and 29 mm in internal diameter. The volume of each sample was maintained at 37 ml, which allowed the vane to penetrate approximately twice its length in the suspension. All tests were performed at  $22 \pm 0.3$  °C.

Stress ramp method was used in this study (Yoon and El Mohtar, 2013a, 2013b). In the technique, a constant level of stress (1 or 3 Pa/step) is maintained for 12 s and the rotation is recorded at the end of the interval before increasing the stress to the next level. The samples were allowed to rest for 2 min after inserting the vane to provide a consistent initial condition by allowing partial recovery of structures disturbed during the insertion. No pre-shearing is applied when investigating the time-dependent change in yield stress from the initial mixing state.

The shear stress ( $\tau$ )–strain ( $\gamma$ ) response was monitored during tests. Initially, the shear stresses increase linearly with increasing strain up to a critical shear stress point after which a significant increase in strain is observed with marginal increase in stress. This critical shear stress point is identified as the yield stress; all yield stresses in this study were determined based on a  $\log \tau$ – $\log \gamma$  plot (Yoon and El Mohtar, 2013a). The time-dependent yield stress measurements were performed at different resting times of 0.5, 1, 24, 48, 120, 240, 480, and 1080 h. While sedimentation of bentonite particles can affect the time-dependent yield stress measurements due to such a long time scale, Yoon (2011) reported that there was no distinct sedimentation of bentonite particles up to 1080 h (45 days). The apparent viscosity values at a high shear rate ( $200 \text{ s}^{-1}$ ) were selected in this study. This shear rate is high enough to compare to expected shear rates during permeation and just low enough for the measurements not to be biased by experimental inertia effects; these effects were particularly observed in suspensions with low bentonite contents and/or high SPP concentrations.

### 2.2.3. ESEM study

The Philips/FEI XL30 ESEM equipment (FEI Company, Hillsboro, OR, USA) was used to examine the network structures in bentonite suspensions with and without SPP. In contrast to the conventional (SEM) equipment, the equipment does not require high vacuum in the specimen chamber; this allowed testing samples under conditions more similar to those in which the sample exists in nature. In this study, a water pressure of 3.9 Torr and the brightness of field emission gun (FEG) of 20 kV were used. After closing the chamber, a vacuum of  $9 \times 10^{-5}$  mBar is applied; the desired accelerating voltage and SE detector are then selected, followed by turning on the filament. Once an image appears, the contrast and brightness are corrected. The 7.5% (1% SPP) suspension was selected for this test over 12% (3% SPP) suspension to observe the microstructures from the close to the initial state. Although the 7.5% suspension is expected to gain lower yield stress with time than 12% suspension, the initial structure of the 7.5% bentonite suspension could not be observed due to the time delay between mixing, sample preparation and capturing the ESEM pictures. Therefore, the ESEM

pictures presented in this study only reflect the relative amount of networks in bentonite suspensions at different resting times.

## 3. Modeling of yield stress build-up with time

The time-dependent yield stress is useful to evaluate post-grouting performance. Previous research (Cambefort, 1977; Axelsson, 2006; Liu and Neretnieks, 2006) showed that the minimum pressure to mobilize a grout inside the pore spaces was proportional to the yield stress of the injected grout. In the proposed application, the pressure to mobilize the placed grout is equal to the external hydraulic stress in the field (Bendahmane et al., 2008). Nguyen and Boger (1985) developed a structural model based on the first order chemical reaction to investigate the recovery of bauxite residue suspensions. Heymann et al. (1996) proposed a similar model for build-up of yield stress in newsprint ink after shearing. Moreover, Leong (1988) proposed a structural recovery model (Eq. (1)) for brown coal suspensions based on the Smoluchowski coagulation theory. In this study, the Leong (1988) model was selected to characterize the effect of SPP on the rate of yield stress build-up with time. This model was chosen because it: (1) is based on the network structures in suspensions, (2) has been validated with Na-montmorillonite-based clay suspensions (de Krester and Boger, 2001), and (3) utilizes one simple parameter to characterize the rate of the yield stress build-up. In this modeling, the yield stress at a given resting time ( $\tau_y(t)$ ) is estimated using the yield stress at infinite time ( $\tau_y^\infty$ ) and the recovery rate parameter,  $K_r$ . However, this model does not capture the increase in yield stresses at short resting times since the model utilizes the second order kinetics, and the predicted values are less accurate for the long resting times because  $\tau_y^\infty$  used in the model must be obtained at a finite time (de Krester and Boger, 2001). The regression analyses utilized by de Krester and Boger (2001) produced significant errors in estimating yield stresses at infinite times due to highly non-linear relationship between  $1/\tau_y$  and  $1/t$ . To overcome this limitation, a root mean square error method was utilized in this study to match the experimental data to the model.

$$\tau_y(t) = \tau_y^\infty \left( 1 - \frac{1 - \left( \frac{\tau_y^\infty}{\tau_y^0} \right)^{3/2}}{1 + K_r t} \right)^{2/3}, \quad (1)$$

where,

|                 |   |
|-----------------|---|
| $\tau_y(t)$     | Yield stress at time $t$                    |
| $\tau_y^\infty$ | Yield stress at time $t \rightarrow \infty$ |
| $\tau_y^0$      | Yield stress at time $t = 0$                |
| $K_r$           | Recovery rate constant (1/time).            |

## 4. Results and discussion

### 4.1. Effect of SPP on initial yield stress and apparent viscosity

Yield stress of 7.5, 10, and 12% suspensions decreases significantly from 27.9, 137.5, and 457.1 Pa to approximately zero with the addition of 2, 3, and 4% SPP, respectively (Figure 1a), implying that the mobility of the suspensions can be significantly improved with a very small amount of SPP (1 to 4% by dry weight of bentonite). At the same 1% SPP concentration, the 7.5% suspension displays approximately 90% reduction in yield stress compared to 50% reduction for the 12% suspension. The addition of more SPP, beyond an optimal threshold, shows a minimal effect on yield stress. For suspensions that do not exhibit a yield stress, the minimum stress ramp step of 1 Pa is assigned as the yield stress. Such suspensions show a linear stress ( $\tau$ )–strain ( $\gamma$ )

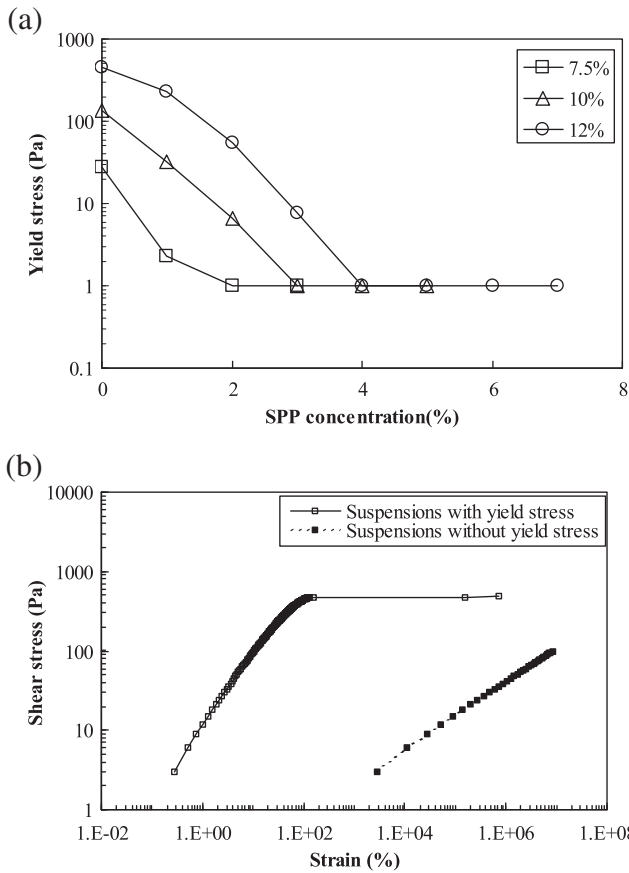


**Fig. 1.** (a) Yield stress of 7.5, 10, and 12% bentonite suspensions with various SPP concentrations (0 to 7%) measured immediately after mixing, and (b) stress–strain curves for the suspensions with and without yield stress (12% bentonite suspensions with 0 and 4% SPP).

curve compared to the bi-linear stress ( $\tau$ )–strain ( $\gamma$ ) curve for suspensions having a yield stress (Figure 1b).

This reduction in yield stress is attributed to the fact that the addition of SPP disrupts the formation of the inter-aggregate bonds (a condensed 3-D network in the concentrated bentonite suspensions which produce a gel state with high yield stress), leading to a liquid state with low to no yield. The phosphate anions are adsorbed on the edge of bentonite particles (or replace the structural hydroxide at the edge), increasing the overall negative surface charge of the particles. This creates a well-developed diffused double layer (Levy et al., 1991) and increases the repulsion forces between the particles, resulting in decreased attractive edge (–) and face (–) (EF) contacts. These repulsive forces reduce the amount of inter-aggregate bonds and, therefore, reducing the 3-D networks in the suspensions (Abend and Lagaly, 2000; Penner and Lagaly, 2001). Once the SPP content is high enough to disrupt the formation of the inter-aggregate bonds (e.g., 2% SPP for 7.5% suspensions), adding more SPP has a minimal effect on the initial yield stress. Suspensions having higher bentonite fractions exhibit more inter-aggregate bonds than the diluted ones and thus, require more SPP to lower the yield stress.

The change in apparent viscosity with shear rate for different bentonite fractions is shown in Fig. 2a. The apparent viscosity increases with bentonite fraction and decreases with shear rate. Since the stress ramp technique is a stress-controlled test, apparent viscosity of the diluted suspensions (and those with high SPP concentrations) could not be measured at low shear rates. While the 12% suspensions at low SPP concentrations (0, 1, and 2%) show viscoelastic responses, an almost purely viscous behavior is observed at the high SPP concentration (3%), indicating that this suspension exhibits more liquid-like behavior (Figure 2b).

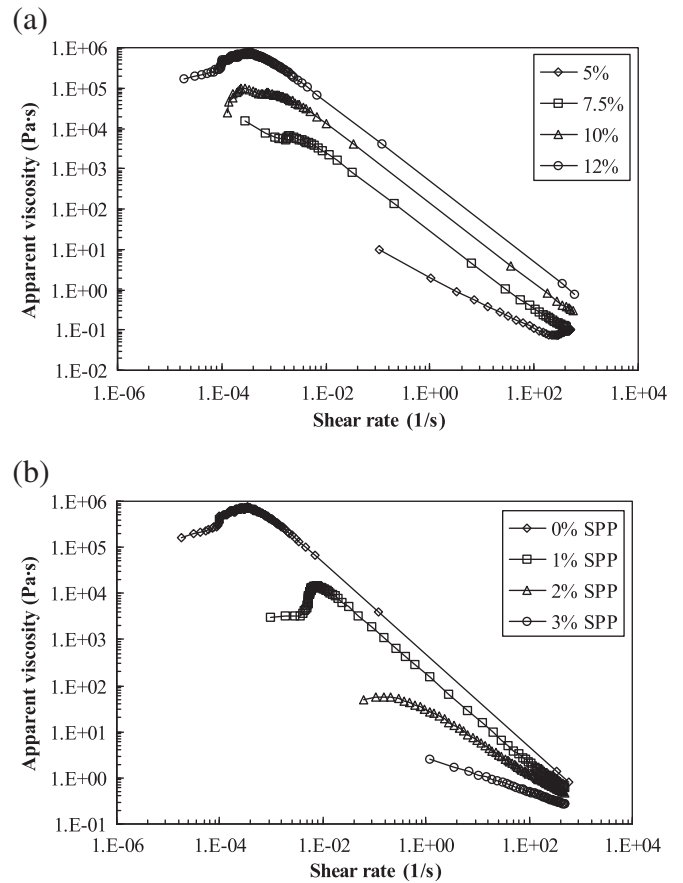


**Fig. 2.** Apparent viscosity of (a) 5, 7.5, 10, and 12% bentonite suspensions, and (b) 12% bentonite suspensions with 0, 1, 2, and 3% SPP concentrations.

The apparent viscosity with various SPP concentrations at a shear rate of  $200 \text{ s}^{-1}$  is shown in Fig. 3. The apparent viscosity of the 7.5, 10, and 12% suspensions is reduced by approximately 66, 86, and 90% by adding 2, 3, and 4% SPP, respectively. The rate of reduction tends to converge as SPP increases because the apparent viscosity becomes a function of the delaminated particle fractions. Therefore, the effect of the SPP on apparent viscosity is limited.

#### 4.2. Time-dependent behavior

The 12% suspensions are mainly utilized to explain the time-dependent rheological behavior of the modified suspensions in this study, while the 7.5, 10, and 12% suspensions are all practically applicable

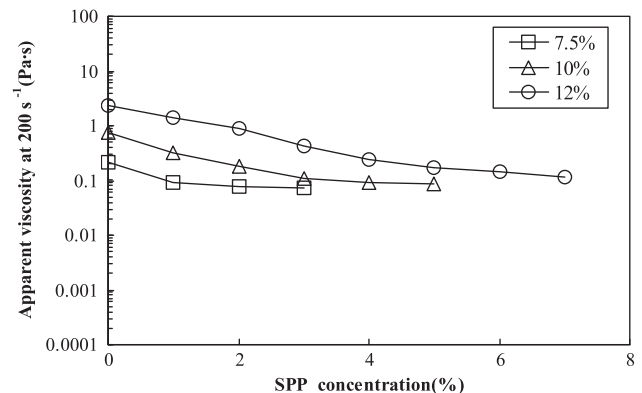


**Fig. 3.** Apparent viscosity of 7.5, 10, and 12% suspensions with SPP concentration (0 to 7%) at shear rate of  $200 \text{ s}^{-1}$ .

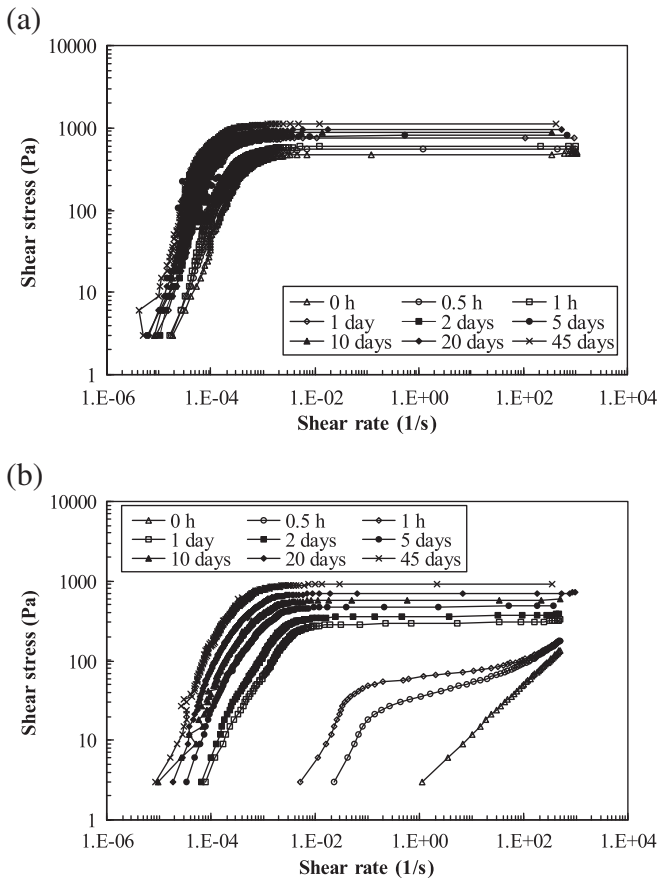


**Fig. 4.** Flow curves for (a) 12% bentonite suspensions, and (b) 12% bentonite suspensions with 3% SPP at the resting time of 0 to 45 days.

depending on design considerations. The flow curves for the unmodified and modified 12% suspensions (Figure 4) at different resting times reveal that the unmodified suspensions show the viscoelastic behavior for all the resting times (gradual increase in shear rate with shear stress followed by a sudden increase in shear rate when the applied stress exceeds yield stress). However, the modified suspensions display a transition from almost pure viscous (no yield stress) to viscoelastic behavior as time elapses. The flow behavior of the modified suspensions changes rapidly even after short resting times (0.5 and 1 h). After approximately 24 h, the modified suspensions show a similar response to the unmodified suspensions. With the increase in resting time, network structures build up, changing the flow behavior from purely viscous to viscoelastic and producing a yield stress. The yield stress increases with resting time, implying that SPP only retards the formation of yield stresses in the bentonite suspensions by delaying the formation of the 3-D networks.

The time-dependent behavior of bentonite suspensions is more clearly shown by investigating the evolution of yield stress at different resting times (Figure 5). Each of the data points shown on the plot is an average of at least three independent measurements on three different samples. On average, the COV (coefficient of variation) is 0.02–0.32, showing a higher COV at short resting times. The yield stress for the 5, 7.5, 10, and 12% suspensions gradually increases from 3.4, 27.9, 135.6, and 457.1 Pa to 40.4, 155.9, 497.7, and 549.5 Pa, respectively, after 45 days (Figure 5a). All suspensions show a linear increase in yield stress with time on a log–log scale (implying a decreasing rate of yield stress buildup with time). The suspensions also show a high increase in yield stress at short resting times, and then the increase in yield stress diminishes as time elapses. The yield stress of the modified suspensions increases with resting time, approaching yield stresses comparable to those of the unmodified bentonite suspension (Figure 5b). The time

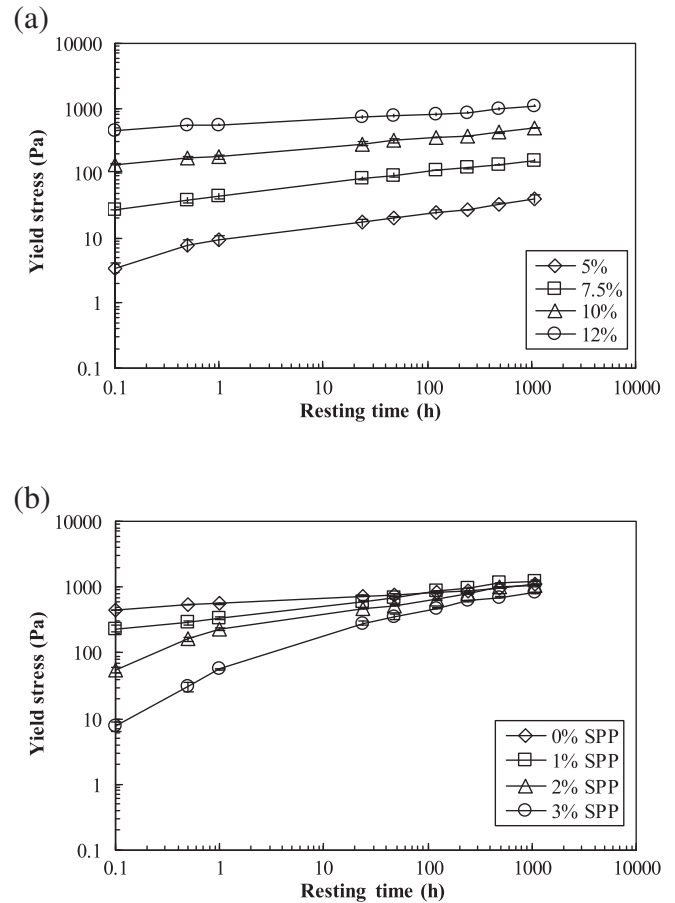


**Fig. 5.** Yield stress evolution for (a) 5, 7.5, 10, and 12%, and (b) 12% suspensions with 0, 1, 2, and 3% SPP at 0 to 45 days.

required, for the yield stresses of the modified suspensions to catch up the yield stresses of the unmodified suspensions, increases with an increase in SPP concentration (5 days for 1% SPP, 20 days for 2% SPP, and greater than 45 days for 3% SPP).

The thixotropy ratio (the ratio of the yield stress at a given resting time to that at a zero resting time) for the different bentonite fractions (Figure 6a) reveals that the thixotropy ratio for the diluted suspensions is larger than that for the concentrated suspensions. Note that the yield stresses of the diluted suspensions are smaller than those of the concentrated suspensions, as shown in Fig. 5a. The time-dependent variation of the thixotropy ratio for the 12% suspensions modified with various SPP concentrations shows that the thixotropy ratio in modified suspensions becomes much larger than those in the unmodified suspensions (Figure 6b). This variation in thixotropy ratio is mostly due to the lower initial yield stress values for the modified suspension while the long-term yield stresses of both, modified and unmodified, are relatively similar.

The increase in the thixotropy ratio depends on the amount of added SPP. Nguyen and Boger (1985) observed a steep recovery of yield stress in bauxite residue suspensions, which was measured from the equilibrium (fully hydrated) condition (>20 h mixing). These results imply that the Brownian motion affects the initial rapid increase in yield stress. As time elapses, the Brownian motion of particles becomes suppressed by the development of network structures. The dependence of the thixotropy ratio on the dispersion concentration also supports that the Brownian motion affects the thixotropy ratio. The increase in the Brownian motion in modified suspensions leads to higher thixotropy ratio due to limited initial network structures. The increase of network structure buildup continues until all the particles assume a minimum free energy (Luckham and Rossi, 1999).

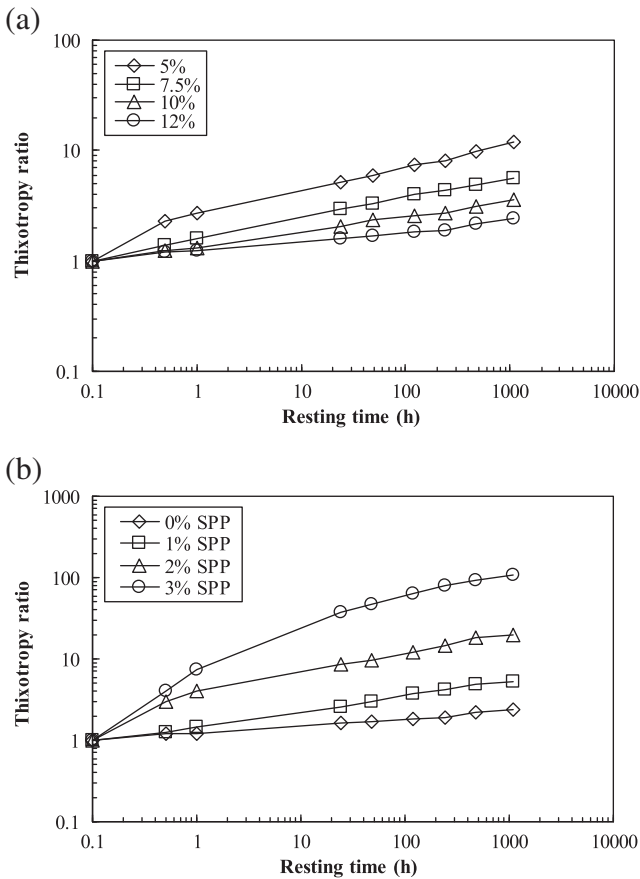


Fig. 6. Thixotropy ratio for (a) 5, 7.5, 10, and 12%, and (b) 12% suspensions with 0, 1, 2, and 3% SPP.

4.3. Effect of hydration on time-dependent behavior

Hydration of bentonite affects the time-dependent behavior of bentonite suspensions, and is important in the proposed application because the mixing method should be determined based on two criteria: 1) significant reduction in the initial flow properties and 2) fast recovery of the reduced properties, especially yield stress. Clem (1985) also reported that the gelling characteristic of bentonite suspensions changed with the presence of the pre-hydration stage in sample preparation. The modified suspensions were prepared by two mixing methods: 1) adding the SPP with the bentonite and water during the initial suspension preparation (the method used through this study), and 2) adding the SPP to the bentonite suspensions after 24 h of pre-hydration and mixing them at a high shear rate of  $500\text{ s}^{-1}$  for 1 min prior to resting for the desired time (0 to 48 h). This high shear mixing after 24 h is assumed to provide similar conditions as the sample preparation mixing while maintaining the full hydration of the bentonite; the resting time for the hydrated specimens is measured from the end of the high shearing stage to the testing time. The comparison of yield stresses from fresh and hydrated 7.5% suspensions shows that the yield stresses of the hydrated suspensions are approximately 10–20% lower than those of the fresh suspensions (Figure 7a). Moreover, the thixotropy ratios in the hydrated suspensions are slightly lower than those of the fresh suspensions, indicating that the recovery is also affected by the degree of the bentonite hydration. For the modified suspensions, the initial yield stresses do not significantly vary with the mixing methods (Figure 7b); the pre-hydrated suspensions show a lower increase in yield stress with resting time (lower thixotropy ratio). However, the thixotropy ratio of both modified suspensions is still greater than that of the unmodified hydrated suspension.

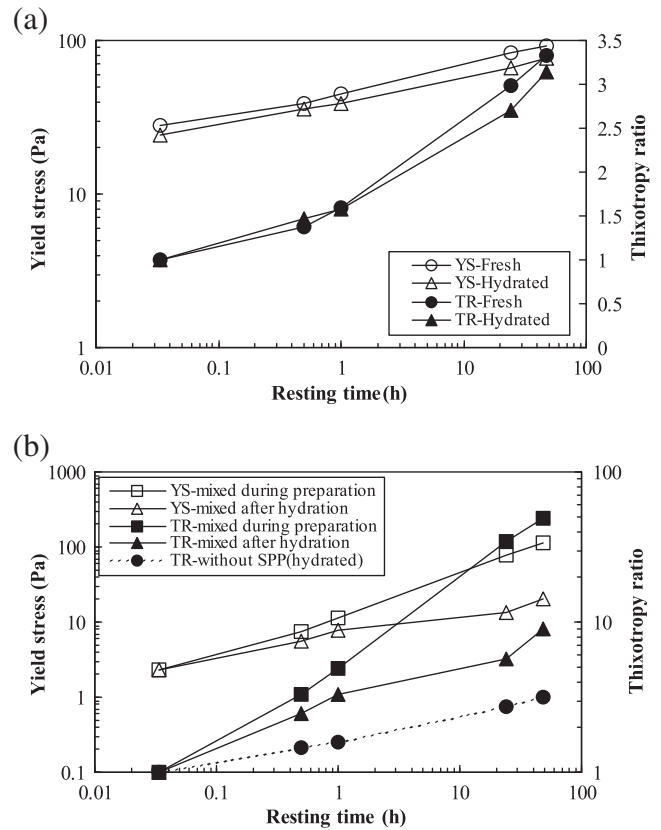


Fig. 7. (a). Yield stress (YS) and thixotropy ratio (TR) of 7.5% bentonite suspensions (fresh and hydrated condition at 0 to 48 h), and (b) yield stress and thixotropy ratio at various resting times (0 to 48 h) with two different mixing methods: 1) addition of SPP during preparation and 2) addition of SPP after hydration of bentonite suspensions for 24 h (for the comparison purposes, thixotropy ratio of the hydrated 7.5% suspensions is shown as well).

For the hydrated bentonite, the adsorption of water molecules between the inter-layers of the clay platelets (the hydration of the exchangeable cations, e.g.,  $\text{Ca}^{2+}$ ,  $\text{Fe}^{3+}$ ...) increases and the attractive forces between the separate platelets are weakened leading to swelling, and thus, a more dispersed suspension (Madsen and Müller-Vonmoos, 1989; Luckham and Rossi, 1999). This swelling produces higher repulsive forces and weak structures formed by the more delaminated platelets. The weak structures are easy to separate under shearing, reducing the yield stress at pre-shearing condition. The degree of separation of bentonite particles highly depends on the amount of cations in bentonite such as calcium and iron ions; bentonite with more ions experiences less separation (Lutz, 1939; Madsen and Müller-Vonmoos, 1989). Without the addition of the SPP, yield stress of bentonite suspension increases with resting time (at rest condition) and decreases (at pre-shearing condition) until hydration (approximately 24 h) stops (Goh et al., 2011). When SPP is added to the hydrated bentonite suspensions, the repulsive forces between the separate platelets increase, leading to a slower buildup of the yield stress.

4.4. Modeling results

The recovery rate parameter ( $K_r$ ) and the predicted yield stresses at infinite time ( $\tau_y^\infty$ ) obtained from this analysis are summarized in Table 3. The recovery rate constant increases as bentonite fraction increases and decreases with an increase in SPP. Increasing the SPP concentration for a given suspension resulted in increasing the characteristic recovery time ( $1/K_r$ ). The comparison of the model with experimental data of 12% suspensions with 0 to 3% of SPP (Figure 8) reveals that the model can capture the overall behavior well. However, discrepancies still existed at

**Table 3**  
Recovery rate constant ( $K_r$ ) and predicted yield stresses at infinite time ( $\tau_y^\infty$ ).

| Parameters                   | $K_r$ (1/h) |       |       |       | Predicted $\tau_y^\infty$ (Pa) |     |     |     |      |
|------------------------------|-------------|-------|-------|-------|--------------------------------|-----|-----|-----|------|
|                              | 5           | 7.5   | 10    | 12    | 5                              | 7.5 | 10  | 12  |      |
| Suspension concentration (%) |             |       |       |       |                                |     |     |     |      |
| SPP concentration (%)        | 0           | 0.011 | 0.018 | 0.019 | 0.020                          | 38  | 148 | 459 | 1024 |
|                              | 1           | N/A   | 0.009 | 0.012 | 0.013                          | N/A | 257 | 708 | 1225 |
|                              | 2           | N/A   | N/A   | 0.009 | 0.011                          | N/A | N/A | 550 | 1071 |
|                              | 3           | N/A   | N/A   | N/A   | 0.007                          | N/A | N/A | N/A | 876  |

N/A indicates “Not Available” because they are not tested.

short resting times due to the limitation of the Leong (1988) model mentioned above. The yield stress at the infinite time increases with a small percentage of SPP and decreases with the increase in the SPP. This is the result of balancing act between two phenomena: 1) the reduced initial network structure with the addition of the SPP and 2) the hydrolysis of SPP that increases the cation concentration in the suspensions (Michaels, 1958). The second phenomenon is more pronounced in the diluted suspensions, resulting in a faster buildup of the network compared to pure bentonite suspensions and strengthens the bonds between particles by suppressing the diffuse double layer.

#### 4.5. ESEM results

Fig. 9a, b, and c are ESEM pictures for the modified 7.5% bentonite suspensions (with 1% SPP) at different resting times (2, 20, and 216 h). The images show the low amount of network structures shortly after mixing; the 3-D network structure becomes more dominant with time in conjunction with the yield stress buildup as measured from the rheological tests. Fig. 9d shows a more prominent 3-D network structure for an unmodified 7.5% suspension after 20 h resting time. The modified suspensions display band-like networks, which produced large flakes and stronger gels (Norrish, 1954; Callaghan and Ottewill, 1974; Duran et al., 2000; Tombácz and Szerkeres, 2004) as compared to the thinner platelets in the unmodified suspension. Kelessidis et al. (2007) observed the similar structures in 6.43% unmodified bentonite suspension. Yoon (2011) reported that the hydraulic conductivities of the Sand–Bentonite Mixtures (SBM) mixed with the modified suspensions were slightly higher than that of SBM mixed with unmodified suspension; this might be explained by the different microstructures of both gels. However, the differences were less than 25%, which is still within the acceptable range of variability in hydraulic conductivity measurements (ASTM D5856). Therefore, the effect of the gel microstructure on hydraulic conductivity of grouted soils is considered to be minimal.

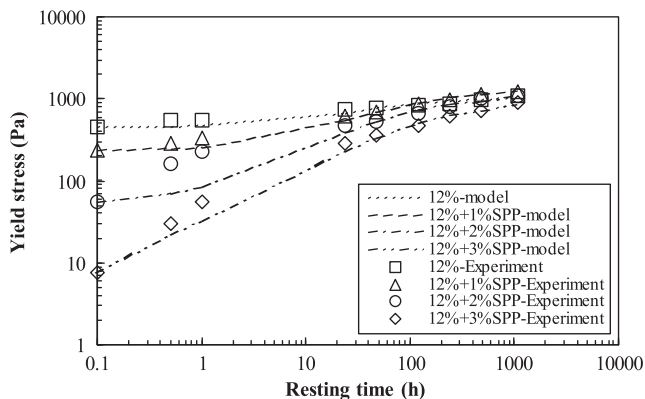


**Fig. 8.** Leong model fitted with experimental data: 12% bentonite suspensions with 0 to 3% SPP.

## 5. Conclusion

The yield stress and apparent viscosity of the modified bentonite suspensions were measured using vane geometry. The addition of a small amount of sodium pyrophosphate (1 to 4%) is found to significantly reduce the yield stress and apparent viscosity of bentonite suspensions. However, this reduction tends to converge after a threshold percentage of SPP (2, 3, and 4% for 7.5, 10, and 12% bentonite suspensions, respectively), indicating that an excessive amount of SPP may not be effective in further reducing the yield stress and apparent viscosity.

The reduced yield stress and apparent viscosity are recovered gradually with resting time. The results show that the hydration of bentonite affects the time-dependent increase in yield stress and thixotropy ratio. The Brownian motion of particles also affects the thixotropy ratio. The concentrated suspensions produce a lower thixotropy ratio than the diluted ones; similarly, larger percentages of SPP show a higher thixotropy ratio at a given resting time. This is possibly because the constrained Brownian motion in the concentrated suspensions produces low thixotropy ratios. On the other hand, the SPP modified suspensions, which show a high degree of Brownian motion due to the reduction of inter-aggregate bonds (3-D networks), produce a higher thixotropy ratio than the unmodified suspensions.

The recovery rate constant of bentonite suspensions was determined based on the Leong model (1988). The recovery rate constant increases with bentonite concentration and decreases with SPP concentration, indicating that the suspensions having high Brownian motion (low bentonite concentration and/or high percentage of SPP) have a slower rate of yield stress buildup than the suspensions having low Brownian motion (high bentonite concentration or low percentage of SPP). The model could capture the overall time-dependent buildup of yield stress in the bentonite suspensions by estimating yield stresses at infinite time from measured data.

In practice, the modified suspensions are injected into soils at low pressures so that the reduction in yield stress is beneficial to increase the penetration distance of grouts. The groutability and maximum penetration distance of particulate grouts (e.g., cement-based suspensions) through porous media are inversely proportional to the apparent viscosity and yield stress of the grout; therefore, the 7.5, 10, and 12% suspensions with 2, 3, and 4% SPP concentrations are practically applicable due to the low apparent viscosity and yield stress. In addition, grouts with lower apparent viscosities will produce lower injection pressures at a given constant rate of injection and reduce the chances of fracturing. Although the SPP is more expensive than other ionic additives, the cost of the proposed SPP percentages is less than 0.3% of the total cost of grouting.

Once the suspensions are injected into the pore space, the yield stress increases over time, thus improving its stability against the external groundwater flow. In order to obtain fast recovery of the reduced yield stress, it is recommended to add the SPP with water and bentonite while the suspension is being prepared. A long-term performance of grouts after being injected into the soil pores can be estimated using the Leong model (1988). However, a complete analysis of the stability of the bentonite grouts within the porous media should account for various factors such as yield stress and apparent viscosity of grouts, soil parameters of the target deposits, and change in hydraulic shear stress exerted by the groundwater flow (e.g., sudden increase of hydraulic gradient in levees during floods). The time-dependent nature of the bentonite suspension also impacts on pumping and workability. Since the increase in yield stress and viscosity of bentonite suspensions is minimal under continuous shearing, its impact on pumping and workability can be minimized through continuous mixing of the suspensions up to pumping time.

These observations support a possible application of the SPP modified bentonite suspensions for seepage control using permeation grouting by (1) increasing penetration distance due to initial reduction

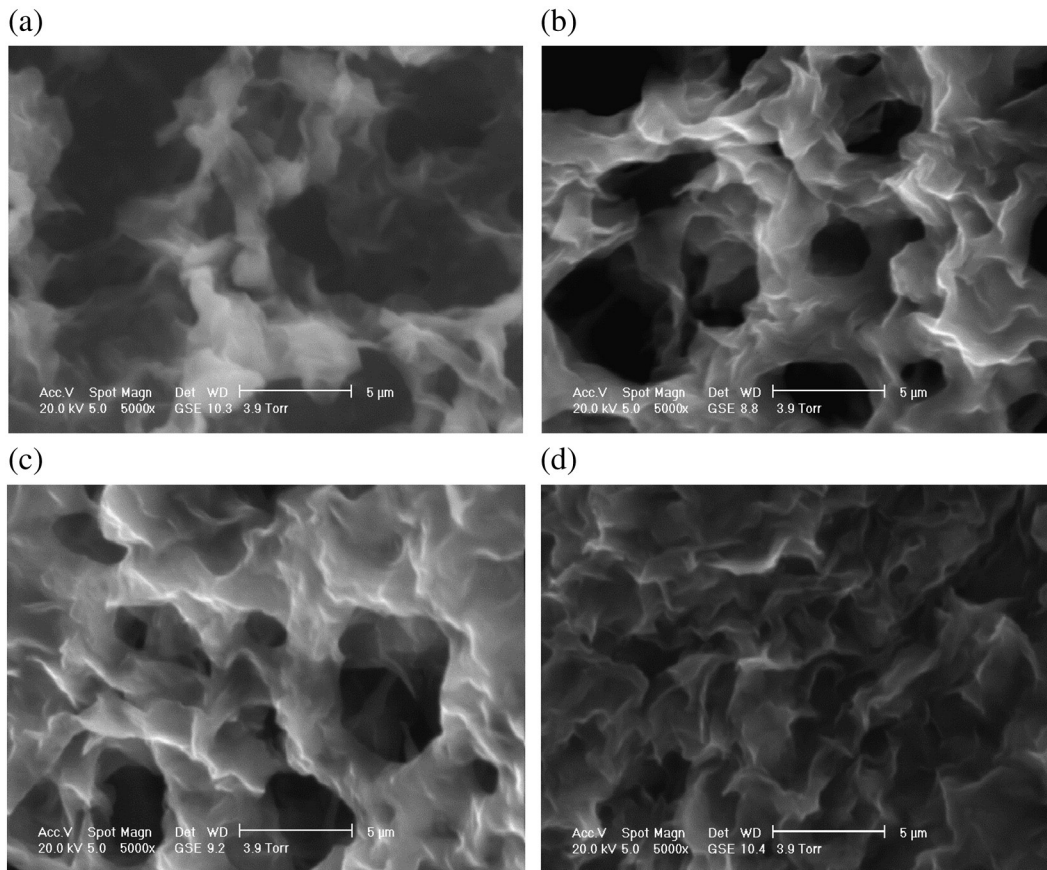


Fig. 9. ESEM pictures of 3-D network in 7.5% bentonite suspensions: (a) 2 h, (b) 20 h, (c) 216 h after mixing (with 1% SPP), and (d) 20 h after mixing (with 0% SPP).

in apparent viscosity and yield stress and (2) reducing the possibility of washout due to the time-dependent increase in yield stress. However, it should be noted that the proposed method should be carefully applied where environmental issues are a major concern. Although no environmental fate and toxicity of the SPP have been reported, the dosage of the SPP may impact on the surrounding environment such as eutrophication of water that promotes algae growth.

### Acknowledgment

This work was partially supported by the National Science Foundation, Geomechanics and Geomaterials program and Geotechnical engineering program, under Grant No. 1254763. This support is gratefully acknowledged.

### References

- Abend, S., Lagaly, G., 2000. Sol–gel transitions of sodium montmorillonite dispersions. *Appl. Clay Sci.* 16, 201–227.
- Alther, G.R., 1987. The qualifications of bentonite as a soil sealant. *Eng. Geol.* 23 (3–4), 177–191.
- Axelsson, M., 2006. Strength criteria on grouting agents for hard rock. Thesis Chalmers University of Technology, Sweden.
- Axelsson, M., Gustafson, G., 2007. Grouting with high water–cement ratios—literature and laboratory study. Report no. 2007:5. Chalmers University of Technology, Sweden.
- Axelsson, M., Gustafson, G., Fransson, A., 2009. Stop mechanism for cementitious grouts at different water-to-cement ratios. *Tunn. Undergr. Space Technol.* 24, 390–397.
- Bendahmane, F., Marot, D., Alexis, A., 2008. Experimental parametric study of suffusion and backward erosion. *J. Geotech. Geoenviron.* 134 (1), 57–67.
- Callaghan, I.C., Ottewill, R.H., 1974. Interparticle forces in montmorillonite gels. *Discuss. Faraday Soc.* 57, 110–118.
- Cambeffort, H., 1977. The principles and applications of grouting. *Q. J. Eng. Geol. Hydrogeol.* 10, 57–95.
- Chegbeleh, L.P., Nishigaki, M., Akudago, J.A., Katayama, T., 2009. Experimental study on ethanol/bentonite slurry injection into synthetic rock fractures: application to seepage control. *Appl. Clay Sci.* 45, 232–238.
- Chrzastowski, M.J., Killely, M.M., Bauer, R.A., DuMontelle, R.B., Erdmann, A.L., Herzog, B.L., Masters, J.M., Smith, L.R., 1994. The great flood of 1993: geologic perspectives on flooding along the Mississippi River and its tributaries in Illinois. Special report 2. Illinois State geological survey.
- Clarke, J.P., 2008. Investigation of Time-Dependent Rheological Behavior of Sodium Pyrophosphate-Bentonite Suspensions Thesis Purdue University.
- Clem, A.G., 1985. Modified bentonite (sodium smectite) sealant membrane. *Eng. Geol.* 21, 327–332.
- de Krester, R.G., Boger, D.V., 2001. A structural model for the time dependent for the mineral suspensions. *Rheol. Acta* 40, 582–590.
- Duran, J.D.G., Ramos-Tejada, M.M., Arroyo, F.J., Gonzalez-Caballo, F., 2000. Rheological and electrokinetic properties of sodium montmorillonite suspensions. *J. Colloid Interface Sci.* 229, 197–217.
- Goh, R., Leong, Y.K., Lehane, B., 2011. Bentonite slurries-zeta potential, yield stress, adsorbed additive and time-dependent behaviour. *Rheol. Acta* 50, 29–38.
- Gonzalez, J., Martin-Vivaldi, J., 1963. Rheology of bentonite suspensions as drilling muds. *Proceedings of the Conference Held at Stockholm, Sweden, August 12–16, 2.* Macmillan, New York, p. 277.
- Gustafson, G., Stille, H., 1996. Prediction of groutability from grout properties and hydrogeological data. *Tunn. Undergr. Space Technol.* 11, 325–332.
- Heymann, L., Noack, E., Kämpfe, L., Beckmann, B., 1996. Rheology of printing inks—some new experimental results. *Proceedings of 12th International Congress on Rheology*, Laval University, Quebec City, Canada, p. 451.
- Hwang, H., Yoon, J., Rugg, D.A., El Mohtar, C.S., 2011. Hydraulic conductivity of bentonite grouted sand. *Proceedings of the Geo-frontiers*, Dallas, TX, pp. 1372–1381.
- Jeong, S.W., 2013. The viscosity of fine grained sediments: a comparison of low- to medium-activity and high-activity clays. *Eng. Geol.* 154, 1–5.
- Jessen, F.W., Turan, F.H., 1961. Deflocculation of fractionated montmorillonite by sodium polyphosphates. *Soc. Pet. Eng. J.* 1, 229–234.
- Kelessidis, V.C., Tsamantaki, C., Dalamarinis, P., 2007. Effect of pH and electrolyte on the rheology of aqueous Wyoming bentonite dispersions. *Appl. Clay Sci.* 38, 86–96.
- Leong, Y.K., 1988. Rheology of Modified and Unmodified Victorian Brown Coal Suspensions Thesis Melbourne University.
- Levy, G.J., Shainberg, I., Alperovitch, N., van der Merwe, A.J., 1991. Effect of N-hexametaphosphate on the hydraulic conductivity of kaolinite–sand mixtures. *Clay Clay Miner.* 39 (2), 131–136.
- Liu, J., Neretnieks, I., 2006. Physical and chemical stability of the bentonite buffer. Report no:R-06-103. Royal Institute of Technology, Sweden.
- Luckham, P.F., Rossi, S., 1999. The colloidal and rheological properties of bentonite suspensions. *Adv. Colloid Interf. Sci.* 82, 43–92.
- Lutz, J.F., 1939. The effect of iron on some physico-chemical properties of bentonite suspensions. *Soil Sci. Soc. Am. J.* 3, 7–12.

- Madsen, F.T., Müller-Vonmoos, M., 1989. The swelling behavior of clays. *Appl. Clay Sci.* 4, 143–156.
- Michaels, A., 1958. Deflocculation of kaolinite by alkali polyphosphates. *Ind. Eng. Chem.* 50 (6), 951–958.
- Mitchell, J., 1993. *Fundamentals of Soil Behavior*, second ed. Wiley, New York.
- Morris, G.E., Žbik, M.S., 2009. Smectite suspension structural behavior. *Int. J. Miner. Process.* 93, 20–25.
- Nguyen, Q.D., Boger, D.V., 1985. Thixotropic behaviour of concentrated bauxite residue suspensions. *Rheol. Acta* 24, 427–437.
- Norrish, K., 1954. The swelling of montmorillonite. *Discuss. Faraday Soc.* 18, 120–134.
- Penner, D., Lagaly, G., 2001. Influence of anions on the rheological properties of clay mineral dispersions. *Appl. Clay Sci.* 19, 131–142.
- Santamarina, J., Klein, K.A., Wang, Y.H., Prencke, E., 2002. Specific surface: determination and relevance. *Can. Geotech. J.* 39, 233–241.
- Seed, R., Bea, R., Abdelmalak, R., Athanasopoulos-Zekkos, A., Boutwell, G., Briaud, J., Cheung, C., Cobos-Roa, D., Ehrensing, L., Govindasamy, A., 2008. New Orleans and hurricane Katrina. I: introduction, overview, and the east flank. *J. Geotech. Geoenviron.* 134 (5), 701–717.
- Tchillingarian, G., 1952. Study of the dispersing agents. *J. Sed. Petrol.* 22, 229–233.
- Tombácz, E., Szerkeres, M., 2004. Colloidal behavior of aqueous montmorillonite suspensions: the specific role of pH in the presence of indifferent electrolytes. *Appl. Clay Sci.* 27, 75–94.
- van Olphen, H., 1977. *An Introduction to Clay Colloid Chemistry*. Wiley, New York.
- Weiss, A., Frank, R., 1961. Über den Bau der Gerüste in thixotropen Gelen. *Z. Naturforsch.* 16, 141–142.
- Yoon, J., 2011. *Application of Pore Fluid Engineering for Improving the Hydraulic Performance of Granular Soils* Ph.D. dissertation The University of Texas at Austin, Austin, TX.
- Yoon, J., El Mohtar, C.S., 2013a. Disturbance effect on time dependent yield stress measurement of bentonite suspensions. *ASTM Geotech. Test. J.* 36 (1), 78–87.
- Yoon, J., El Mohtar, C.S., 2013b. Groutability of granular soils using sodium pyrophosphate modified bentonite suspensions. *Tunn. Undergr. Space Technol.* 37, 135–145.
- Yoon, J., El Mohtar, C.S., 2013c. Dynamic rheological properties of sodium pyrophosphate modified bentonite suspensions. *Clay Clay Miner.* 61 (4), 319–327.
- Yukselen, Y., Kaya, A., 2008. Suitability of the methylene blue test for surface area, cation exchange capacity and swell potential determination of clayey soils. *Eng. Geol.* 102, 38–45.